A new very high-order finite volume method for the 2D convection diffusion problem on unstructured meshes

Stéphane Clain, Gaspar Machado, Rui M. S. Pereira

A new very high-order finite volume method for the 2D convection diffusion problem on unstructured meshes

Stéphane Louis Clain[1,2], Gaspar J. Machado[1], and Rui M. S. Pereira[1]

[1]Universidade do Minho, DMA and CMAT, Campus de Azurém, Guimarães, Portugal
email: clain@math.uminho.pt http://sites.google.com/site/clain00/
[2] Université Paul Sabatier, Institut de Mathématique de Toulouse, Toulouse, France

Abstract

We present a new finite volume scheme based on the Polynomial Reconstruction Operator (PRO-scheme) for the linear convection diffusion problem with structured and unstructured meshes. We first design the numerical scheme for generic two-dimensional cells and introduce two kinds of polynomial reconstructions. Numerical experiences are carried out to prove the stability and the effectiveness of the method where a 6th-order convergence is reached.

Key-words: *Finite volume scheme; polynomial reconstruction; high-order scheme; convection diffusion.*

1 INTRODUCTION

Numerical approximations of steady-state convection-diffusion problem are a constant challenge, namely the design of robust and efficient numerical schemes, whatever the Peclet number is (pure convection or pure diffusion). Classical and popular method such as the finite element or the finite difference methods are usually adopted to perform numerical approximation and their efficiency is well-known. Nevertheless, such methods suffer of several withdraws. First, since we evaluate point-wise approximations or its representation on a finite element basis, continuity of the solution is mandatory. In the finite volume framework, discontinuous solutions are also available since we consider mean values on cells. Another important aspect is the conservation property; the finite volume method has the built-in local conservation property whereas such a property is not guaranteed in the finite element or finite difference context.

Finite volume method has been mainly developed for hyperbolic problems as Euler system, Shallow Water, pure convection problems. Since the early eighties, the book of Patankar [1] was a constant reference in the framework of finite volume methods for structured meshes. In the two last decades, efforts have been done to propose efficient scheme for elliptic or parabolic problems where the conservation property is mandatory. Techniques such as the Diamond Cell method [2] and the DDFV method [3, 4] have been introduced, and a mathematical analysis of such method is done in [5]. Unfortunately, most of the schemes are at most second-order scheme and suffer of strong numerical diffusion reducing the approximation accuracy. Very few methods in the elliptic context reach very high accuracy [6, 7] (we mean more than the second-order). We propose a new class of numerical schemes to provide very high-order approximation for the steady-state convection diffusion problem with two-dimensional geometries and unstructured meshes. The two ingredients are, on the one hand, a polynomial reconstruction operator [8, 9] which produces local polynomial representations of degree 5 for each cell, and on the other hand, a finite volume method based on the local polynomial representations. The technique has been successfully tested for one-dimensional geometry [10] and we generalize it for the more complex 2D situation.

The paper is structured as follows. Section 2 presents the convection-diffusion problem we shall deal with and the geometrical ingredients we need to build the scheme. Section 3 is devoted to the Polynomial Reconstruction Operator which is the key-point of the method. We present in Section 4 the finite volume scheme. Numerical tests are presented in Section 5 to show the effectiveness of the method.

2 THE NUMERICAL PROBLEM

Let consider an open bounded domain $\Omega \subset \mathbb{R}^2$ with boundary $\partial\Omega = \Gamma_D \cup \Gamma_N$. We consider the classical convection diffusion problem

$$-\nabla.(a\nabla u) + \nabla.(Vu) = f \text{ in } \Omega, \quad u = u_d \text{ on } \Gamma_D\ ;\ a\nabla u.n - uV.n = g \text{ on } \Gamma_N,$$

where $a(x, y)$ stands for the diffusion coefficient, $V(x, y) = (v_1, v_2)$ represents the velocity and n the outward normal vector on the boundary (see Fig. 1).

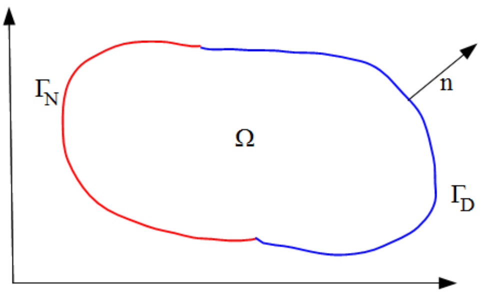

Figure 1 – Computational domain with Neumann and Dirichlet condition on the boundary.

Let us denote by T a mesh constituted of polyhedral cells c and by $e = c|c'$ the edge which shares two cells c and c'. We introduce the sets $\mathcal{C}$ and $\mathcal{E}$ as the collection of all the cells and all the edges respectively. Sets $\mathcal{E}_O$, $\mathcal{E}_D$ and $\mathcal{E}_N$ represent the inner edges and the edges on Γ_D and Γ_N, respectively. For each cell c, we denote by

$$\nu(c) = \{c' \in \mathcal{C}; c' \cap c \in \mathcal{E}_O\}.$$

In the same way, we denote by $S(c)$ a collection of cells associated to the generic cell c named the stencil. Note that $S(c)$ is different of $\nu(c)$ but we shall require that $\nu(c) \subset S(c)$ for the sake of consistency. In the same way, for any edge $e \in \mathcal{E}_D$, $S(e)$ is a stencil constituted of cells belonging to the neighborhood of edge e. To conclude the section, we highlight that in the finite volume framework the number of unknowns is equal to the number of cells, namely $I = \#\mathcal{C}$ and we shall denote by u_i an approximation of the mean value on cell c_i, $i = 1, \dots, I$.

3 THE POLYNOMIAL RECONSTRUCTION OPERATOR (PRO)

For a given function u defined on domain Ω, u_d on Γ_D and g on Γ_N, we denote by $< u >_c$ the mean value of u on cell c, by $< u_d >_e$ the mean value of the Dirichlet condition on edge $e \in \mathcal{E}_D$, and by $< g >_e$ the mean value of the Neumann condition on edge $e \in \mathcal{E}_N$. In particular, for any cell $c \subset \Omega$ of centroid B or any edge $e \subset \partial\Omega$ of midpoint B, we define the mean values of the polynomial function $(X - B)^\alpha = (x - B_x)^{\alpha_1}(y - B_y)^{\alpha_2}$ of degree $\alpha = (\alpha_1, \alpha_2)$ on the cell or on the edge by

$$< (X-B)^\alpha >_c = \frac{1}{|c|}\int_c (X-B)^\alpha dxdy, \qquad < (X-B)^\alpha >_e = \frac{1}{|e|}\int_e (X(s)-B)^\alpha ds$$

respectively, where $X(s)$ is a parameterization of edge e, and $|c|$ and $|e|$ stand for the measure of the cell and the edge, respectively. We shall consider two kinds of polynomial reconstruction: the conservative and the non-conservative one.

3.1 Conservative reconstruction

Let us give a set of values u_i, $i = 1, \dots, I$. We present two conservative reconstructions, one for the cells and the other for the edges. Let $c \in \mathcal{C}$ be a reference cell and $S(c)$ the associated stencil. We consider the generic conservative polynomial reconstruction of degree d on cell c

$$\hat{u}_c(x,y) = u_c + \sum_{1 \le |\alpha| \le d} \Re_\alpha \left[(x - B_x)^{\alpha_1} (y - B_y)^{\alpha_2} - M_\alpha \right]$$

where $|\alpha| = \alpha_1 + \alpha_2$ and $M_\alpha =< (X - B)^\alpha >_c$. The term conservative comes from the fact that by construction one has $< \hat{u}_c >_c = u_c$ which means that we preserve the mean value over the reference cell.

Coefficients $\Re_\alpha$ are determined by a least squares method with respect to the mean values on neighboring cells providing polynomial function $\hat{u}_c(x,y)$. To this end we introduce the functional

$$\hat{\mathrm{E}}_c(\Re) = \sum_{c' \in S(c)} \omega_{c'} \left[u_{c'} - \frac{1}{|c'|} \int_{c'} \hat{u}_c(x,y) dxdy \right]^2$$

where $\omega_{c'}$ are the positive weights associated to the functional and denote by $\hat{\Re}_\alpha$ the coefficients of the polynomial which minimizes $\hat{\mathrm{E}}_c(\Re)$. From a practical point of view, one has to solve an over-determined system where the matrix is only composed of geometrical issues performing a QR Householder decomposition to quickly solve the underlying least square problem.

We proceed in the same way with the edge. Let $e \in \mathcal{E}_D$ be a reference edge and $S(e)$ the associated stencil, we consider the generic conservative polynomial reconstruction of degree d on cell c

$$\hat{u}_e(x,y) =< u_d >_e + \sum_{1 \le |\alpha| \le d} \Re_\alpha \left[(x - B_x)^{\alpha_1} (y - B_y)^{\alpha_2} - M_\alpha \right],$$

which preserves the mean value on the edge and introduce the similar functional

$$\hat{\mathrm{E}}_e(\Re) = \sum_{c' \in S(e)} \omega_{c'} \left[u_{c'} - \frac{1}{|c'|} \int_{c'} \hat{u}_e(x,y) dxdy \right]^2 .$$

Coefficients $\Re_\alpha$ are determined by a least squares method with respect to the mean values on neighboring cells as before.

3.2 Non-conservative reconstruction

Let $e \in \mathcal{E}_O$ be an inner edge. Since we do not compute any approximation on the edge (except for the Dirichlet condition), the conservative polynomial reconstruction does not make sense in this case since no mean value should be associated to edge e. Consequently, we introduce the non-conservative form namely

$$\tilde{u}_e(x,y) = \sum_{0 \le |\alpha| \le d} \Re_\alpha \left[(x - B_x)^{\alpha_1} (y - B_y)^{\alpha_2} \right].$$

Note that the sum start at 0 since the constant term is also an unknown. As previously, we determine the coefficients minimizing the functional

$$\tilde{E}_e(\mathfrak{R}) = \sum_{c' \in S(e)} \omega_{c'} \left[u_{c'} - \frac{1}{|c'|} \int_{c'} \tilde{u}_e(x,y) dxdy \right]^2$$

and we denote by $\widetilde{\mathfrak{R}}_\alpha$ the coefficients of the polynomial which minimizes $\tilde{E}_e(\mathfrak{R})$. Note that in both cases, one must have $\#S(c)$ and $\#S(e)$ greater than $\frac{d(d+1)}{2}$ to obtain an over-determined system.

4 THE FINITE VOLUME SCHEME

Based on the polynomial reconstruction operator, we define the numerical convective and diffusive fluxes on edges $e \in \mathcal{E}$ where we denote by q_e^r the Gauss points on the edge and ζ^r the associated weight, $r = 1,2,3$. We warn the reader to well-distinguish conservative reconstruction $\hat{u}$ with the non-conservative one $\tilde{u}$. We have to distinguish three situations with regard the the inner or boundary edges.

- If $e = c|b \in \mathcal{E}_O$, we define the flux from cell c toward cell b (direction $n_{c|b}$) as

$$\mathcal{F}_{c|b,r} = [V(q_e^r).n_{c|b}]^- \hat{u}_b(q_e^r) + [V(q_e^r).n_{c|b}]^+ \hat{u}_c(q_e^r) - a(q_e^r)\nabla\tilde{u}_e(q_e^r).n_{c|b}.$$

- If $e \in \mathcal{E}_D$ in an edge of cell c, we define outward the flux from cell c (direction n_c) as

$$\mathcal{F}_{e,r} = [V(q_e^r).n_{c|b}]^- u_d(q_e^r) + [V(q_e^r).n_{c|b}]^+ \hat{u}_c(q_e^r) - a(q_e^r)\nabla\hat{u}_e(q_e^r).n_{c|b}.$$

  Note that we use the Dirichlet condition for the inflow contribution and the conservative reconstruction for the diffusive part.

- If $e \in \mathcal{E}_N$ in an edge of cell c, we just set $\mathcal{F}_{e,r} = g(q_e^r)$.

To define the finite volume scheme we introduce the G_c operator. Consider a vector $U = (u_i)_{i=1,\dots,I}$ where each component u_i is an approximation of the mean-value on cell c_i, we then built all the associated polynomial reconstructions presented in the previous section and we define the operator

$$g_i = \sum_{b \in S(c_i)} \sum_{r=1,2,3} \omega_r |c_i| \mathcal{F}_{c_i|b,r} + \sum_{\substack{e \in \mathcal{E}_D \\ e \subset c_i}} \sum_{r=1,2,3} \omega_r |e| \mathcal{F}_{e,r} - \sum_{\substack{e \in \mathcal{E}_N \\ e \subset c_i}} \sum_{r=1,2,3} \omega_r |e| g(q_e^r) - |c_i| < f >_{c_i}.$$

Note that the known contribution (source term and Neumann condition) are introduced with the minus sign since we put all the balance equation terms on the left-side. Therefore, for a given vector $U \in \mathbb{R}^I$, we define the affine operator $G_c(U) = (g_1, g_2, \dots, g_I) \in \mathbb{R}^I$ and the steady-state solution $\overline{U}$ satisfies the equation $G_c(\overline{U}) = 0$.

Since the operator is affine, there exists a matrix A and a vector b such that $G_c(U) = AU - b$. Note that we do not know explicitly the associated matrix A and the right-hand side term b since we deal with a constructive procedure: form U we compute the polynomial reconstruction, then the fluxes, then operator $G_c(U)$. To solve the system, we consider two ways. A first approach consists in computing numerically the matrix and the right-hand side noting that $b = -G_c(0)$and $A_i = G_c(E_i) + b$ where E_i is the vector of the canonical basis with *i*-component equal to 1. Such a way is computational heavy but provides the full matrix and allows the eigenvalues analysis (positivity) and the conditioning number calculation. The alternative consists in applying an iterative routine such as GMRES, since the method only requires the computation of the residual which is exactly operator $G_c(U)$.

5 NUMERICAL TESTS

To check the numerical schemes effectiveness, we have carried out several numerical tests to compute the convergence rate of the method. The academic unit square Ω domain is meshed with cells (triangles or quadrilaterals) to provide a discretization T_I with respect to number I of cells. For a given solution u, we denote by u_i the mean value approximation on cell c_i while $< u >_{c_i}$ is the exact mean value. We introduce two types of errors: the L_1 and L_∞ errors given by

$$E^\infty = \sup_{c_i \in C} |u_i - < u >_{c_i} |, \qquad E^1 = \sum_{c_i \in C} |u_i - < u >_{c_i} ||c_i|.$$

5.1 A pseudo-1D test

We first consider a problem where we impose the solution invariant with respect to y (pseudo 1D case). To this end, a pure diffusive problem with diffusion coefficient equal to 1 is investigated. Let Γ_D and Γ_N be the vertical and horizontal border respectively and set $u(x, y) = \sin(2\pi x)$, we easily check that function u is the unique solution of

$$-\Delta u = f, \;\; u = 0 \;\text{ on } \Gamma_D, \qquad \frac{\partial u}{\partial n} = 0 \;\text{ on } \Gamma_N$$

with $f = 4\pi^2 \sin(2\pi x)$ as the source tem. We perform numerical simulations and compute errors in the L_1 (left) and L_∞ (right) norms employing several types of reconstruction and first deal with unstructured meshes. We use uniform weights for the convective reconstruction associated to each cell (one for all). For the diffusive flux based on the edges, we use a weight equal to 3 for the two cells sharing the edge while the other weights are equal to one.

Table 1: Errors in the $\mathbf{L_1}$ (left) and $\mathbf{L_\infty}$ (right) norms for three types of reconstructions: P1, P3, and P5.

I	h e-02	PRO-P1				PRO-P3				PRO-P5			
		L_1-err	ord	L_∞-err	ord	L_1-err	ord	L_∞-err	ord	L_1-err	ord	L_∞-err	ord
88	10.660	1.09e-01	—	3.00e-01	—	1.56e-02	—	7.86e-02	—	2.44e-03	—	1.57e-02	—
202	7.036	3.74e-02	2.6	1.06e-01	2.5	2.50e-03	4,40	9.75e-03	5.0	2.52e-04	5.5	1.02e-03	6.6
578	4.159	9.59e-03	2.6	5.15e-02	1.4	2.64e-04	4.27	9.64e-04	4.4	9.62e-06	6.2	5.24e-05	5.7
1038	3.104	4.71e-03	2.4	2.24e-02	2.8	7.74e-05	4.29	3.30e-04	3.7	1.93e-06	5.5	1.17e-05	5.1
1816	2.347	2.75e-03	1.9	1.46e-02	1.5	2.20e-05	4.51	1.78e-04	2.2	2.49e-07	7.3	2.53e-06	5.5

We plot in Table 1 the error and the convergences rates for the L_1 and L_∞ norms. For the L_1 norm, we obtain a second-order convergence with PRO-P1, a fourth-order convergence with PRO-P3 and a sixth-order convergence with PRO-P5 as expected. Note that for the last mesh (1816 cells) the L_1 errors ratio between the P1 and P5 reconstructions is around 11000! With the L_∞ norm, convergence rates are not so straight for the following reason: the L_∞ norm is very restrictive since a unique value with larger error is enough to destroy the convergence rate. In practice, we have observed that only 1% of cells present an error of order to the L_∞ norm while the other cells have an error of order to the L_1 norm. Just very few cells present a larger error. Currently, we do not know which mechanism is responsible of the extra error (matrix resolution, stencil, weight?).

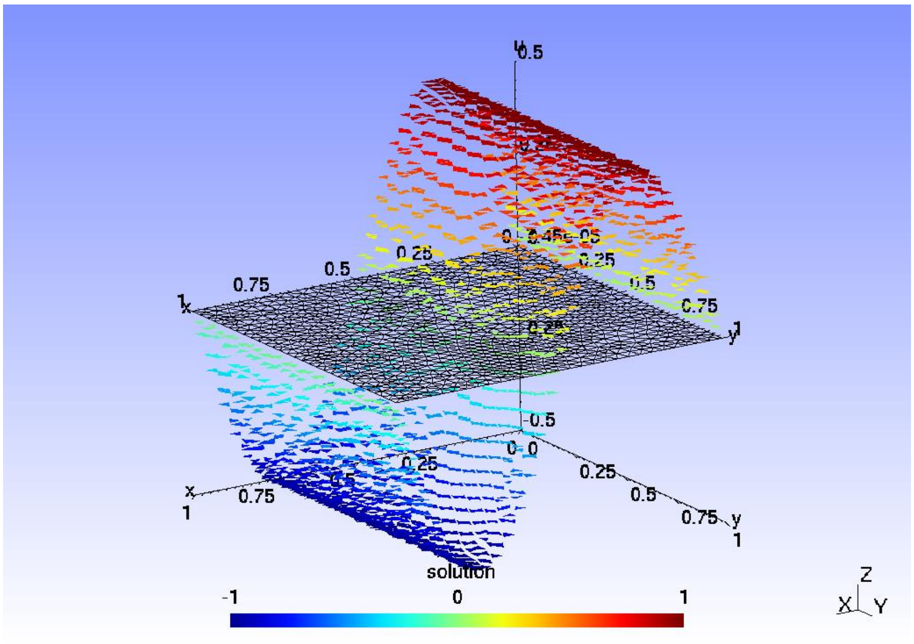

Figure 1: Numerical approximation with an unstructured mesh.

Figure 1 shows the approximation computed on an unstructured mesh while Figure 2 provides the convergence curves using the L_1 (left) and L_∞ (right) norms in log-scale graph. We observe a regular decreasing of the error and the excellent convergence rate with the PRO-P5 method.

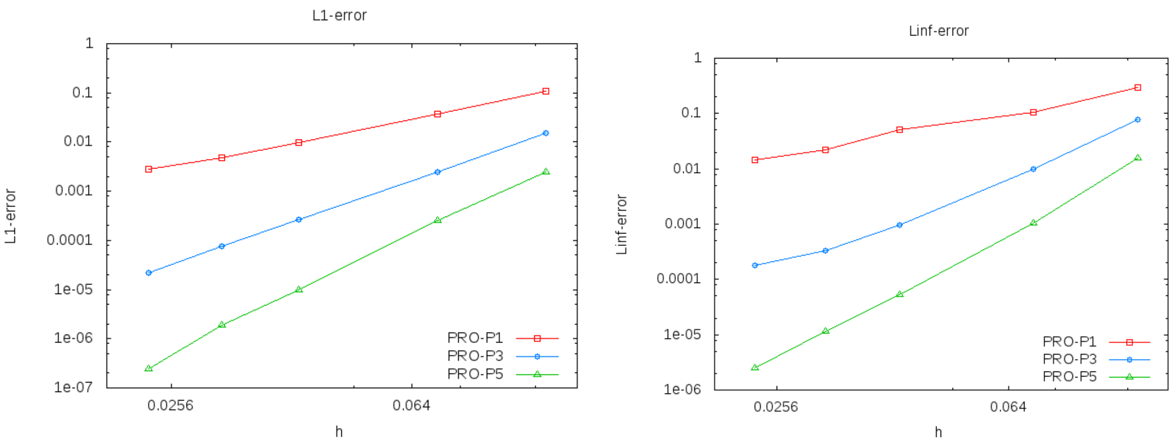

Figure 2: Unstructured meshes case. Convergence rates in the L_1 (left) and L_∞ (right) norms.

We now turn to the case where we employ structured meshes in order to compare with the unstructured version. We have meshed the domain with quadrilateral elements to provide a uniform grid very similar to the ones use for a 1D configuration. As in the previous case, we use uniform weights for the convective reconstruction associated to each cell. For the diffusive flux based on the edges, we use a weight equal to 3 for the two cells sharing the edge while the other weights are equal to one.

Table 2: Errors in the $\mathbf{L_1}$ (left) and $\mathbf{L_\infty}$ (right) norms for three types of reconstructions: P1, P3, and P5.

I	h e-02	PRO-P1				PRO-P3				PRO-P5			
		L_1-err	ord	L_∞-err	ord	L_1-err	ord	L_∞-err	ord	L_1-err	ord	L_∞-err	ord
90	10.54	1.46e-01	—	5.27e-01	—	1.96e-02	—	6.37e-02	—	4.65e-03	—	1.33e-02	—
182	7.412	6.09e-02	2.49	1.69e-01	3.23	4.12e-03	4.42	1.40e-02	4.30	7.28e-04	5.27	3.43e-03	3.85
380	5.219	2.77e-02	2.14	8.15e-02	1.98	7.68e-04	4.56	4.09e-03	3.35	6.45e-05	6.59	3.17e-04	6.46
756	3.636	1.28e-02	2.44	3.91e-02	2.14	1.68e-04	4.41	1.05e-03	3.96	8.16e-06	6.01	4.52e-05	5.67
1560	2.532	6.25e-03	1.98	2.08e-02	1.74	4.08e-04	3.91	2.98e-04	3.47	7.78e-07	6.48	5.32e-06	5.91

We plot in Table 2 the error and the convergences rates for the L_1 and L_∞ norms. As in the structured case, we obtain the expected convergence rate but this time both for the two norms with a slight degradation for the L_∞ norms. One more time, only few cell present (less than 1%) presents a larger error. Note that for the last mesh (1560 cells) the L_1 errors ratio between the P1 and P5 reconstruction is around 8000!

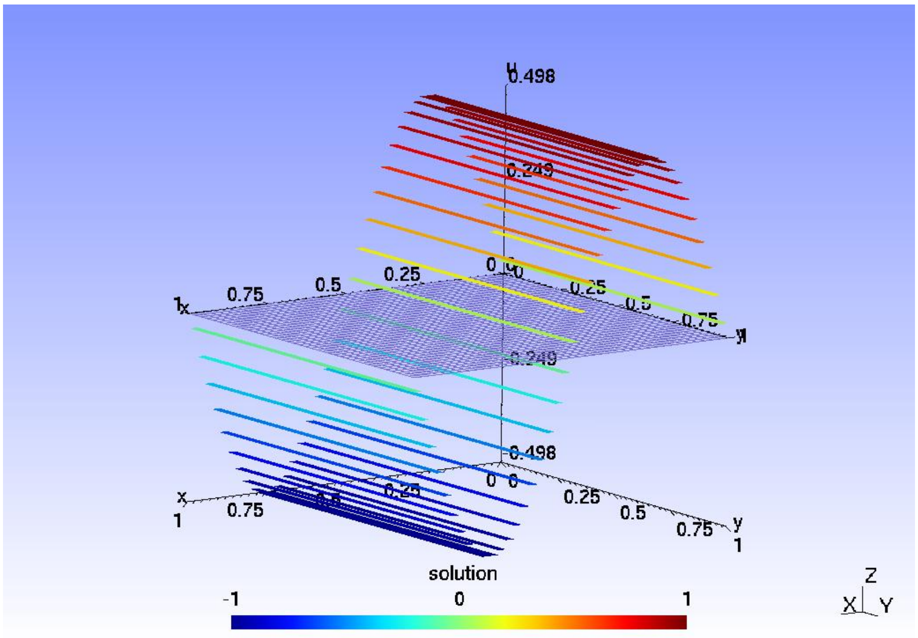

Figure 3: Numerical approximation with a structured mesh

Figure 3 shows the approximation computed on a structured mesh while Figure 4 provides the convergence curves using the L_1 (left) and L_∞ (right) norms in log-scale graph. We also observe a regular decreasing of the error and the excellent convergence rate with the PRO-P5 method. Note that the performance is very similar to the unstructured case.

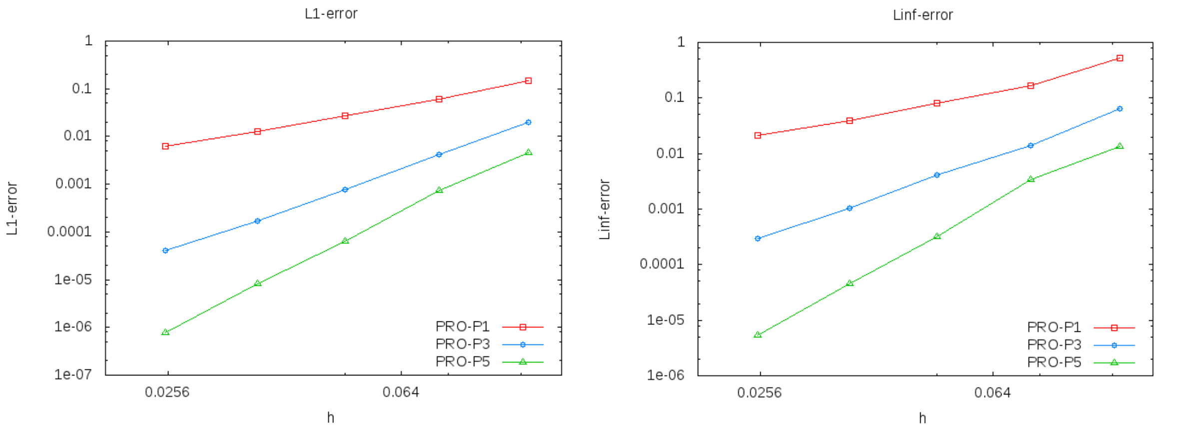

Figure 4: Structured meshes case. Convergence rates in the L_1 (left) and L_∞ (right) norms.

5.2 A full 2D test

For a given constant velocity $V = (V_x, V_y)$, we introduce the following functions:

$$\alpha(x) = \frac{1}{V_x}\left(x - \frac{e^{xV_x} - 1}{e^{V_x} - 1}\right), \quad \beta(y) = \frac{1}{V_y}\left(y - \frac{e^{yV_y} - 1}{e^{V_y} - 1}\right).$$

One can easily check that function $u(x,y) = \alpha(x)\,\beta(y)$ is the solution of the steady-state convection diffusion problem with $a = 1$, $f(x,y) = \alpha(x) + \beta(y)$ and homogeneous Dirichlet condition on the whole boundary. We perform numerical simulations and compute errors with the two norms for several meshes. We use uniform weights for the convective reconstruction associated to each cell. For the diffusive flux based on the edges, we use a weight equal to 3 for the two cells sharing the edge while the other weights are equal to 1.

Table 3: Errors in the $\mathbf{L_1}$ (left) and $\mathbf{L_\infty}$ (right) norms for three types of reconstructions: P1, P3, and P5.

I	h e-02	PRO-P1				PRO-P3				PRO-P5			
		L_1-err	ord	L_∞-err	ord	L_1-err	ord	L_∞-err	ord	L_1-err	ord	L_∞-err	ord
104	9.806	4.71e-04	—	2.12e-03	—	3.10e-05	—	1.49e-04	—	2.87e-06	—	1.14e-05	—
230	6.594	3.17e-04	1.0	1.36e-03	1.1	5.25e-06	4.5	5.68e-05	2.4	2.60e-07	6.1	1.52e-06	5.0
452	4.703	2.11e-04	1.2	9.66e-04	1.0	1.78e-06	3.2	1.97e-05	3.1	6.14e-08	4.2	4.46e-07	3.6
946	3.251	9.39e-05	2.2	4.79e-04	1.9	4.85e-07	3.5	6.89e-06	2.8	6.13e-09	6.2	5.25e-08	5.8
1928	2.277	2.72e-05	3.4	2.42e-04	1.9	1.01e-07	4.4	2.23e-06	3.2	6.47e-10	6.3	9.10e-09	4.9

We plot in Table 3 the error and the convergences rates for the L_1 and L_∞ norms. We obtain with the L_1 norm a second order-scheme for the PRO-P1, a fourth-order convergence rate with the PRO-P3 and a sixth-order rate with the PRO-P5. As mention above, the discrepancy with the L_∞ norm derives from an extra error for a few cells. Note that for the last mesh (1928 cells) the L_1 errors ratio between the P1 and P5 reconstruction is around 33000!

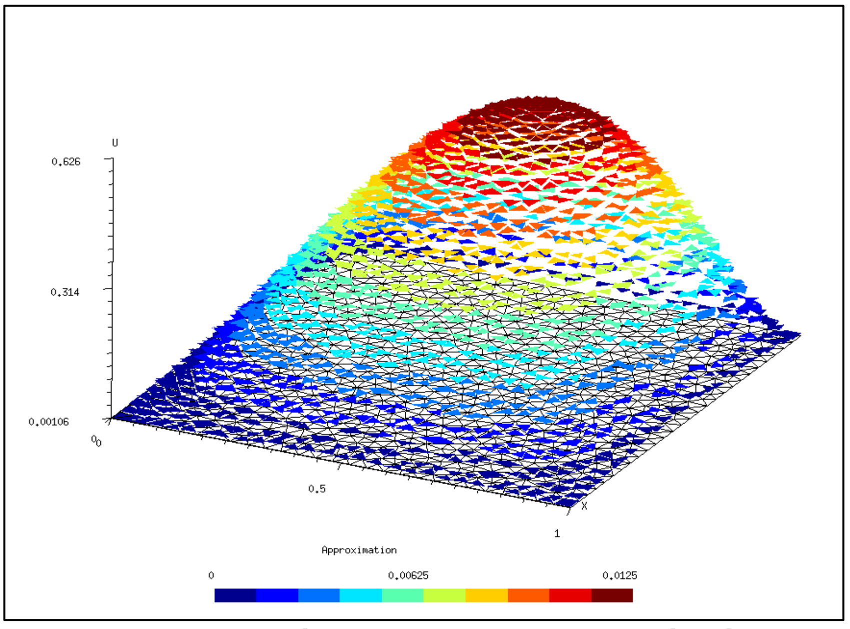

Figure 5: numerical approximation on an unstructured mesh.

We plot in Figure 5 the mesh with the approximate solution while the convergence curves are printed in Figure 6. As in the previous cases (pseudo-1D) we recover very good effective convergence rates with order very close to the expected (theoretical) ones.

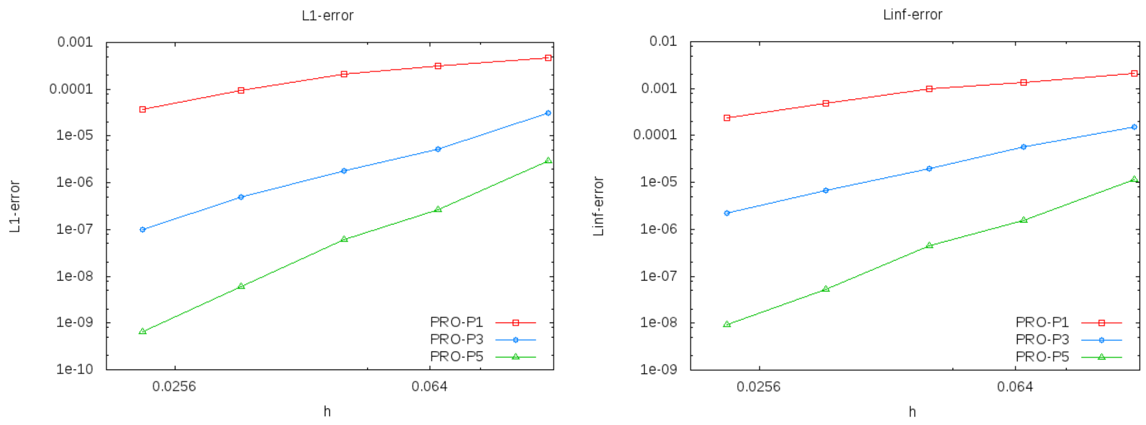

Figure 6: Convergence rates in the L_1 (left) and L_∞ (right) norms.

6 CONCLUSION

In this short paper, we have presented a new finite volume method to provide very high-order approximation for the steady-state convection diffusion problem. We show effective convergences for simple examples using structured or unstructured meshes to prove the efficiency of the method. Lots of things remain to be done to provide a competitive method with respect to the classical ones (namely the finite element method), especially to reduce the error in L_∞ norm, i.e., eliminate the few cell which provide an extra error. Non-stationary versions are under studies while a 3D version is a further goal.

7 ACKNOWLEDGEMENTS

This research was financed by FEDER Funds through Programa Operacional Factores de Competitividade — COMPETE and by Portuguese Funds through FCT — Fundação para a Ciência e a Tecnologia, within the Project PEst-C/MAT/UI0013/2011 and the project PTDC/MAT/121185/2010.

REFERENCES

1. S. V. Patankar, *Numerical Heat Transfer and Fluid Flow*, Series in Computational Methods in Mechanics and Thermal Sciences, McGraw Hill, (1980).

2. Y. Coudière, J.P. Vila, and P. Villedieu, Convergence rate of a finite volume scheme for a two dimensional convection diffusion problem, *Modél. Math. Anal. Numér*. 33 (3) (1999), pp. 493—516.

3. G. Manzini and A. Russo, A finite volume method for advection-diffusion problems in convection-dominated regimes, Comput. Methods Appl. Mech. Engrg. 197 (2008), pp. 1242—1261.

4. K. Domelevo and P. Omnes, A finite volume method for the Laplace equation on almost arbitrary two-dimensional grids, *M2AN Math. Model. Numer. Anal*. 39 (2005), pp. 1203—1249.

5. R. Eymard, T. Gallouët, and R. Herbin, *The finite volume method*, *Handbook for Numerical Analysis*, Ph. Ciarlet J.L. Lions eds., North Holland, (2000), pp. 715—1022.

6. E. F. Toro and A. Hidalgo, ADER finite volume schemes for nonlinear reaction-diffusion equations, *Applied Numerical Mathematics archive* 59 (1) (2009), pp. 1—31.

7. C. Ollivier-Gooch and M. Van Altena, A high-order-accurate unstructured mesh finite-volume scheme for the advection-diffusion equation, *Journal of Computational Physics Archive* 181 (2) (2002), pp. 729—752.

8. S. Clain, S. Diot, R. Loubère, A high-order polynomial finite volume method for hyperbolic system of conservation laws with Multi-dimensional Optimal Order Detection (MOOD), *Journal of computational Physics*, 230 (2011), pp. 4028—4050.

9. S. Clain, S. Diot, R. Loubère, Improved detection criteria for the Multi-dimensional Optimal Order Detection (MOOD) on unstructured mesh with very high-order polynomials. To be published *in Computers & Fluids* (2012).

10. S. Clain, G. Machado, R. Pereira, R. Ralha, S. Diot, R. Loubère, Very high-order finite volume method for one-dimensional convection diffusion problems, Mathematical Models for Engineering Science (MMES'11), in Puerto De La Cruz, Tenerife, Spain, December (2011).